



Activated carbon fibres as high performance supercapacitor electrodes with commercial level mass loading

Manavalan Vijayakumar, Ravichandran Santhosh, Jyothirmayi Adduru,
Tata Narasinga Rao, Mani Karthik*

International Advanced Research Centre for Powder Metallurgy and New Materials (ARCI), Balapur, Hyderabad, 500005, India

ARTICLE INFO

Article history:

Received 3 June 2018

Received in revised form

8 August 2018

Accepted 26 August 2018

Available online 29 August 2018

ABSTRACT

Turning waste cotton into useful energy storage device shows great scientific and industrial importance due to the sustainability, abundance, low-cost and environmental friendliness. This study delineates the fabrication and electrochemical performances of activated porous carbon fibres used as high performance supercapacitor electrodes with commercial level mass loading ($150 \pm 10 \mu\text{m}$ thickness, $10 \pm 1 \text{ mg cm}^{-2}$). The fabricated supercapacitor electrodes showed combination of high gravimetric and volumetric capacitances in three different electrolytes 6 M KOH (0–1 V), 0.5 M Na₂SO₄ (0–1.8 V) and 1 M TEABF₄/AN (0–2.7 V) due to the thick electrodes (high active mass loading). Particularly, the electrodes in organic electrolyte TEABF₄ at 2.7 V exhibited excellent gravimetric and volumetric capacitances of 112 F g^{-1} and 74 F cm^{-3} at 1 A g^{-1} , respectively with long life cycle (87% capacitance retention after 10,000 cycles). Hence, it delivers maximum gravimetric and volumetric energy density of 29.50 Wh kg^{-1} and 19.42 Wh L^{-1} , respectively. A practical approach to combine the supercapacitor (4 coin cells in series, 2.7 V x 4) with commercial solar lantern to integrate self-sustaining power pack is demonstrated. It is evidently proved that activated carbon fibres with high areal capacitance delivered high volumetric energy to the device which is prime requisite for practical implementation.

© 2018 Elsevier Ltd. All rights reserved.

1. Introduction

The design and development of alternative energy storage technologies with cost-effective, environmental friendliness and sustainability of the devices are strongly needed in order to reduce the fossil fuel consumption as well as to reduce the environmental pollution [1,2]. The effective methods to store electrical energy for use on demand are critical issues [3,4]. Electrical Energy Storage (EES) is recognised as great potential technologies in meeting these challenges, whereby energy is stored in a certain state, according to the technology used, and is converted into electrical energy when needed [5,6]. Among the various energy storage technologies, supercapacitors (SCs) and lithium batteries (LiB) are at the frontier of the research [7,8]. SCs and LiB devices as representative modern energy storage devices have been widely utilised in our daily life by powering various portable electronic devices and even current plug

in hybrid electric vehicles [9,10]. In this concern, electrochemical energy storage systems, including batteries and electrochemical supercapacitors, designed for energy storage are especially favoured because they are sustainable and eco-friendly [11–13].

Among these, supercapacitors have been recognised as promising next generation energy storage devices due to their ultra-fast charging time, very high power density, and long cycle life as compared than most widely used lithium ion batteries in the commercial applications [14–27]. At the same time, low energy density and high production cost of supercapacitor as compared with lithium ion batteries are restricted their practical applications, which need to be addressed [28,29]. These drawbacks can be mitigated by developing a new class of high performance premium grade supercapacitor carbon electrodes which consists of a combination of materials produced from abundant, cheap, environmentally friendliness and sustainable resources with low processing costs [30,31].

Besides, the active mass of the electrodes is considered as major influence parameters on the electrochemical performances [32]. In order to construct the supercapacitor with an optimize energy density or power density, the supercapacitor electrodes are made

* Corresponding author.

E-mail addresses: mkarthik@project.arcires.in, [\(M. Karthik\).](mailto:karthik_annauni@yahoo.co.in)

with the thickness of about 100–200 µm [33]. The less active mass of the electrode or thin electrode can always lead to an overstatement of a material's performance because, on the one hand, the significant errors could be possible during the measurement of active mass of the electrode when handling and weighing the microgram sized electrodes, and on the other hand, the signal to noise (S/N) ratio is also the major concern [34,35]. For reliable electrochemical measurements, a supercapacitor electrode should have a thickness and active mass similar to the commercial electrodes i.e. 100–200 µm and 10–12 mg cm⁻², respectively [36,37]. In the view of above, the active mass of the electrodes with commercial level of loading should be investigated on the electrochemical performances for practical validity.

To explore the renewable resources, cotton is considered as a natural sustainable carbon-rich precursor for the synthesis of carbon materials owing to their low cost, environmental friendliness and scalability. In the light of the above, we introduce waste cotton as renewable carbon precursor that might have promising applications for supercapacitors in the near future. India is the largest producers of cotton with 2nd position in the world and accounting for about 26% of the world cotton production. The waste cotton can be recycled and reused for several applications. In the present study, the waste cotton was used as a carbon source because of its low cost, easy availability and biodegradable nature. Cotton is a soft and fluffy fibre which contains almost pure cellulose as polysaccharide. Cotton can be considered as a suitable carbon source for supercapacitor applications because it contains only the polysaccharide which converts into pure carbon upon carbonisation at above 600 °C under N₂ atmosphere. Generally, other biomass carbon sources are containing several elemental/mineral compositions those are retained after carbonisation even at high temperature up to 1000 °C and the final elemental composition like metals, metal oxides and ashes should be removed by purification process which often causes the expensive process as well as environmental threats.

It is very important and essential to design and fabricate the cost effective, green and clean process for manufacturing the supercapacitor device for commercial applications. In the present contribution, we demonstrate a large scale preparation of high surface area activated carbon fibres (ACF, 1550 m²/g) derived from waste cotton as an economic abundant renewable natural resource and the fabrication of high-performance supercapacitor device was examined by using different electrolytes such as 6 M KOH (0–1 V), 0.5 M Na₂SO₄ (0–1.8 V) and 1 M TEABF₄/AN (0–2.7 V). The electrochemical performance and supercapacitive behaviours of carbon fibres electrodes with commercial level mass loading are investigated and the salient results are discussed. The schematic representation of the overall concept of biomass waste cotton conversion into green energy storage is illustrated in Fig. 1.

2. Experimental section

2.1. Fabrication of activated porous carbon fibers

High surface area porous carbon fibres derived from waste cotton was obtained by pre-carbonisation followed by chemical activation. Briefly, the waste cotton obtained from cotton industry (Jansons Industries Ltd, Tiruchengode, Tamilnadu, India) was pre-carbonized by using a tubular furnace under N₂ flow at 600 °C for 1 h with a rate of heating 5 °C min⁻¹ and the carbon yield from the pre-carbonisation of waste cotton is around 25 wt %. After pre-carbonisation, the resulting carbon powder was mixed with potassium hydroxide (KOH) in the weight ratio of 1:3, respectively. Then, the above mixture was placed in the alumina crucible and kept in the stainless steel tube within a tubular furnace. The

activation of carbon sample was carried out at 850 °C for 1 h with a rate of heating 5 °C min⁻¹ under N₂ flow. The resulting activated carbon sample was washed thoroughly with distilled water up to neutral pH. Then, the carbon sample was dried for 12 h at 100 °C. Cotton fibres are composed of 100% cellulose and it is converted into 100% carbon upon carbonisation without any impurities.

2.2. Characterization of the materials

The surface morphologies of the materials were analysed by using scanning electron microscopy (SEM-Hitachi SU-70, Japan) and transmission electron microscopy (TEM Model: FEI Tecnai G-20,200 KeV). The elemental mapping and composition of the activated samples were analysed by using Energy Dispersive X-ray Analysis (EDAX). X-ray diffraction (XRD) measurement was carried out by using Bruker AXS D8 advance system using Cu K α radiation ($\lambda = 1.5406 \text{ \AA}$) in the range of $2\theta = 10\text{--}80^\circ$ at room temperature. X-ray photoelectron spectroscopy (XPS) analysis was performed by using ESCA-Omicron XPS with Mg K α as the excitation source. The surface area (SA), pore diameter and pore volume of the carbon samples were characterised by N₂ adsorption–desorption isotherms at 77 K using a Micromeritics, ASAP 2020 surface area analyser. Prior to the measurements, the carbon samples were degassed under vacuum (10^{-3} mbar) at 250 °C for 8 h. The pore size distributions were obtained by utilising 2D-NLDFT as reported in our previous report [38,39].

2.3. Electrodes preparation and electrochemical measurements

The carbon–carbon electrodes were fabricated by mixer of 90 wt % of active material (activated carbon fibres) and 10 wt % of binder (Polyvinylidene Fluoride-PVDF). The mixture was homogenised by adding a few drops of N-Methyl-2-pyrolidone (NMP) and then a uniform slurry was obtained. The disk-shaped identical self-standing two electrodes of 12 mm in diameter were prepared and weighed. The thickness of electrodes and the corresponding mass loading of the electrodes per cm² were controlled and then the final thickness about $150 \pm 10 \mu\text{m}$ and the mass loading of the electrodes about $10 \pm 1 \text{ mg cm}^{-2}$ were fixed. Finally, carbon–carbon symmetric supercapacitor were prepared by using two identical carbon electrodes, a porous membrane separator (glass fibre), and two stainless steel current collectors (SS316S) assembled in a Teflon Swagelok® cell in 6 M KOH and 0.5 M Na₂SO₄. The coin cell assembly was used for 1 M TEABF₄/AN organic electrolyte.

The electrochemical performances such as charge-discharge, cyclic voltammetry and electrochemical Impedance were recorded by using potentiostatic electrochemical work station (Solartron SI-1287 and Princeton Applied Research - Ametek) with a two-electrodes configuration at different current densities. For galvanostatic charge-discharge and CV measurements, the potential windows of 0 V–1 V for 6 M KOH electrolyte, 0 V – 1.8 V for 0.5 M Na₂SO₄ and 0 V – 2.7 V for 1 M TEABF₄/AN organic electrolyte were used.

Specific capacitance is the capacitance per unit mass for one electrode. The specific capacitance of the supercapacitor electrodes were calculated from the discharge curves by using equation (1) [40].

$$C_{sp} (\text{F/g}) = 4^* \text{ C/m} \quad (1)$$

Cell capacitance is measured from galvanostatic or constant current (CC) discharge curves using equation (2) [40].

$$C = I / (dV/dt) \quad (2)$$

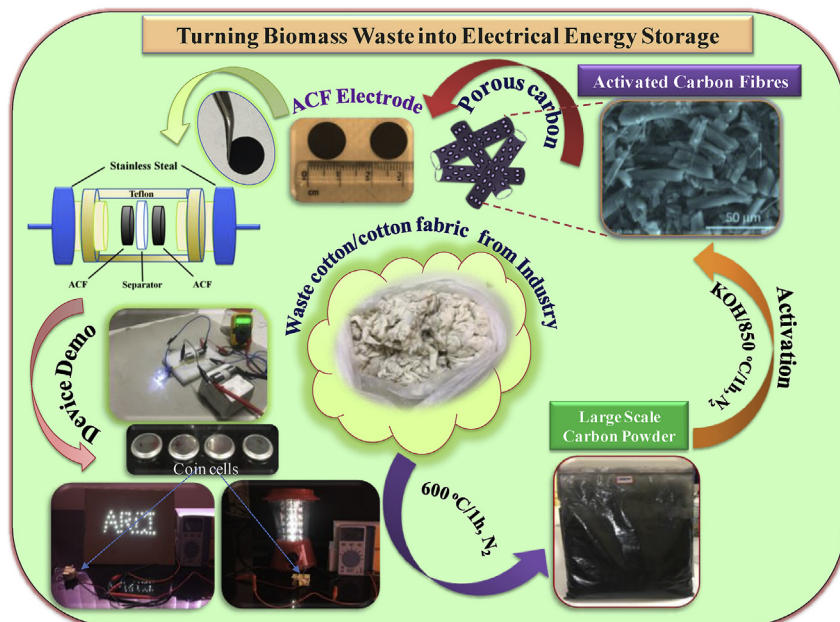


Fig. 1. Schematic representation of turning biomass waste conversion into green energy storage. (A colour version of this figure can be viewed online.)

Where, C_{sp} - specific capacitance of the electrode; C - measured capacitance for the two-electrodes cell; m (g) - the active mass of the both electrodes without binder mass; I (A) - the discharge current; dV (V) - the total potential window and dt (s) - the discharge time, respectively.

The energy and power densities of the two symmetrical supercapacitor electrodes were calculated by using equations (3) and (4):

$$E (\text{Wh/kg}) = 1/2 C_{sp} V^2 \quad (3)$$

$$P (\text{W/kg}) = \frac{E}{\Delta t} \quad (4)$$

Where, C_{sp} - the specific capacitance of the symmetrical supercapacitor (Fg^{-1}) calculated from equation (1), V (V) refers to the potential change of galvanostatic discharge process, Δt (s) is discharge time.

Ion diffusion coefficient (D) was calculated according to the straight line at low frequencies of Nyquist plots based on equations (5) and (6) [41]:

$$D = \frac{R^2 T^2}{2A^2 n^4 F^4 C^4 \sigma^2} \quad (5)$$

$$Z_{RE} = R_s + R_{ct} + \sigma \omega^{-1/2} \quad (6)$$

In the above two equations, R , T , A , n , F , C , R_s , R_{ct} and σ correspond to gas constant, room temperature, surface area of the electrode, the electron numbers that ion transferred, Faraday constant, ohmic resistance, charge transfer resistance, the ion's concentration and the slope Z_{RE} against $\omega^{-1/2}$, respectively.

3. Results and discussion

3.1. Textural characteristics of the activated porous carbon fibres

The textual properties such as specific surface area (BET), specific pore volume and average pore size of the activated carbon

fibres were derived from N_2 adsorption-desorption measurements as depicted in Fig. 2. The BET isotherm clearly exhibited a type I isotherm according to the IUPAC classification, which reflects the microporous nature and the initial portion of the isotherm at low P/P_0 values corresponds to micropore volume filling [38–40]. It can be observed that there is no hysteresis between the adsorption and desorption branches which indicates the saturation of isotherm. This feature indicates the presence of typical microporous materials. T-plot results also showed that the micropore volume and specific surface area of carbon are estimated to be $0.69 \text{ cm}^3 \text{ g}^{-1}$ and $1550 \text{ m}^2 \text{ g}^{-1}$, respectively. The pore size distribution of the carbon fibres is depicted in Fig. 2 (inset) and it showed a narrow pore size distribution with an average pore diameter of 1.3 nm. The high specific surface with narrow pore size of the obtained activated carbon fibres electrode can offer sufficient electrode-electrolyte interaction to form electric double layers.

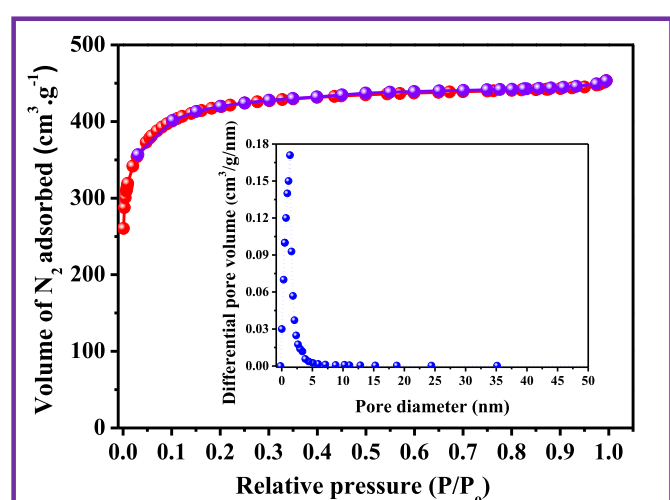


Fig. 2. Nitrogen adsorption-desorption isotherm of activated carbon fibres (Inset: BJH pore size distribution). (A colour version of this figure can be viewed online.)

The surface morphology of the carbon fibres before and after activation was examined by using SEM as shown in Fig. 3. The fibre morphology of the parent cotton/cotton fabric is well preserved even after carbonisation. The parent cotton mainly consists of cellulose fibres with diameters between 10 and 20 μm . After pre-carbonisation, cellulose fibres are converted into thin carbon fibres after shrinkage with the average diameter of around 8–10 μm . Fig. 3(a) shows the direct conversion of cotton fabric into carbon fabric upon carbonisation at 600 °C for 1 h. After KOH activation, the carbon fibres are broken into several small fragmentations but it retains fibres morphology as depicted in Fig. 3(d–f). It is believed that KOH activation is creating substantial and very uniform micropores on the surface of the carbon fibres as evidenced by BET-BJH pore size measurement. The well retained fibre morphology with highly microporous structure is essential and important for the supercapacitor application because it can provide very good pathway not only for the electrolyte penetration but also electrolyte ion transfer. Besides, the interconnected macroporous fibre

network can also provide the uniform and good electrical conductivity throughout the supercapacitor electrode.

In order to determine the crystalline structure and surface elemental compositions of activated carbon fibers (ACF), XRD and XPS measurements were performed as depicted in Fig. S1 and S2. XRD pattern of ACF sample exhibit two broad peaks at ca. 25° and ca. 44°, which can be indexed as (002) and (101) reflections of typical amorphous nature of the carbon, respectively. XPS spectra show the presence of carbon (C1s) with a small amount of oxygen (O1s) elements and the corresponding concentrations of the C and O elements are 95 at. % and 5 at. %. XPS result confirmed that there are no other impurities in the ACF. C1s scans show three peaks at around 284.33, 285.7 and 288.3 eV which corresponding to C=C/C–C in sp²-hybridized domains, C–O (epoxy, hydroxyl), and O=C–O (carboxyl) groups, respectively [42]. O1s scans show two peaks at 531.95 and 530.49 eV, pointing out the existence of quinone and carboxyl group, respectively [42]. These oxygen-containing functional groups on the surface of the carbon can

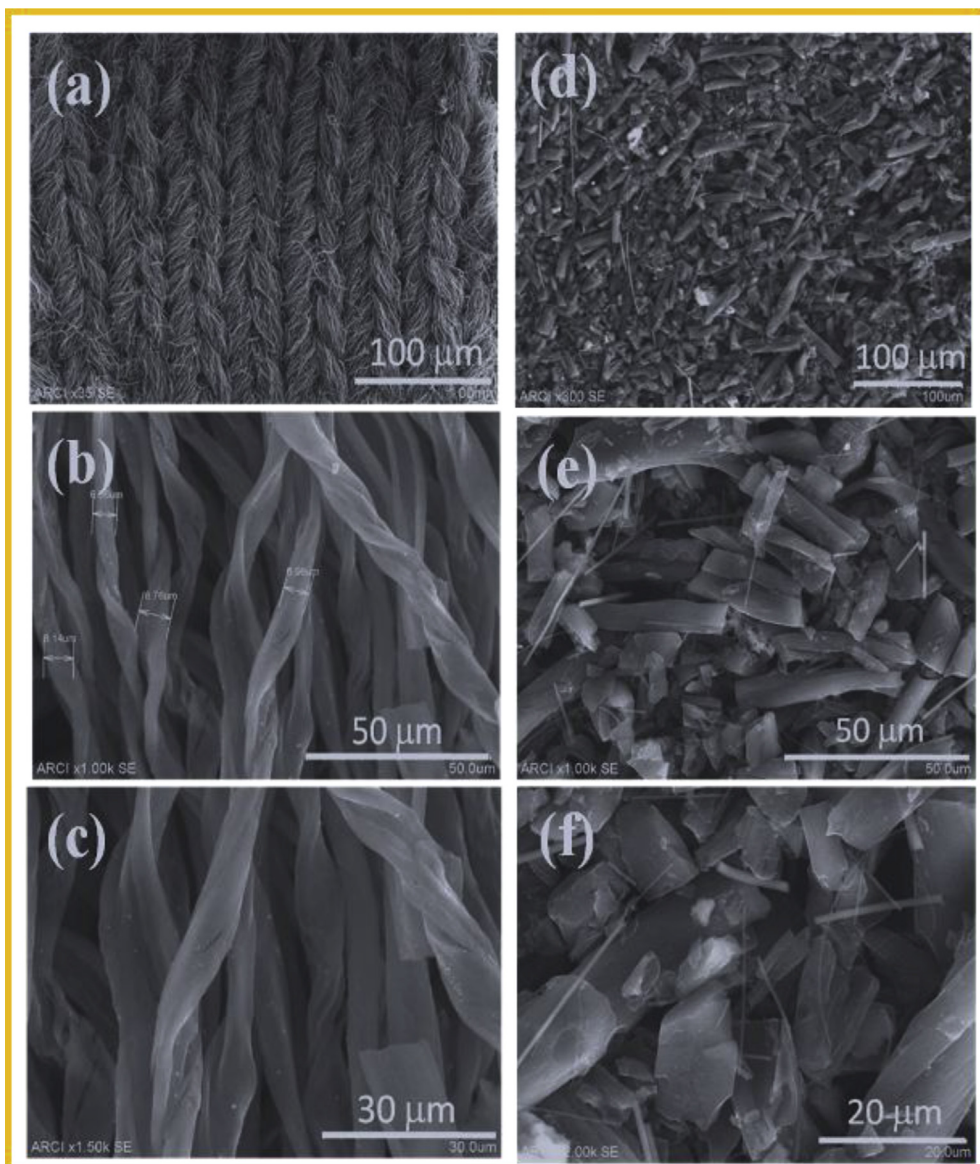


Fig. 3. Surface morphology of the carbon fibres before and after KOH activation: (a–c) SEM images of carbon fibres before activation, (d–f) SEM images of carbon fibres after activation. (A colour version of this figure can be viewed online.)

modify the polarity of the carbon surface that can further promote the wettability between carbon surface and electrolyte which is important for the double layer formation.

3.2. Electrochemical performance

Based on the above characteristics of the activated carbon fibres, it is anticipated that the high surface area with narrow pore size distribution and fibrous morphology of the activated carbon fibres may exhibit good electrical double layer capacitor (EDLC) performance. In order to evaluate the practical electrochemical energy storage performance of activated carbon fibres, two symmetric supercapacitor electrodes were fabricated by using different electrolytes such as aqueous 6 M KOH, neutral 0.5 M Na₂SO₄ and organic 1 M TEABF₄ electrolytes. Generally, a typical commercial supercapacitor cell is comprised of two electrodes that are isolated from electrical contact by a porous separator. For reliable electrochemical measurements, a supercapacitor electrode should have a thickness and active mass similar to the commercial electrodes i.e. 100–200 µm and 10–12 mg cm⁻², respectively [43–45]. Hence, the thickness of electrode and the corresponding mass loading of the electrode per cm² were controlled and then the final thickness ca. 150 ± 10 µm and the mass loading of the electrode ca. 10 ± 1 mg cm⁻² were fixed because it is prerequisite to compare the electrochemical performance with the commercial electrodes.

It is worthy to mention here that the electrode with high amount of the active mass can store more energy and hence it has higher areal capacitance, which is very important for commercial applications. The energy storage performance of the supercapacitor electrodes were investigated by using cyclic voltammetry (CV), galvanostatic charge-discharge (GCD) and electrochemical impedance spectroscopy (EIS). In order to understand the diffusion rate of the electrolyte ions in the supercapacitor electrodes, cyclic voltammetry test was performed at various sweep rates. Charge-discharge test was performed at various current densities. These two tests were utilised to study the electrochemical evaluation of the supercapacitors performance of the synthesised activated carbon fibres. Supercapacitor cells were assembled in different electrolytes, with various potential windows from 0 to 1 V for KOH electrolyte, 0–1.8 V for Na₂SO₄ electrolyte, and 0–2.7 V for 1 M TEABF₄ electrolyte, respectively. The CV curves of the electrode under different voltage window of 0.5 M Na₂SO₄ as well as 6 M KOH electrolytes were examined at the scan rate of 20 mV s⁻¹ and the results are shown in Fig. 4. It is worthy to mention here that the scan rate of 20 mV s⁻¹ is selected for the comparison because the voltage sweep rates of at minimum of 20–40 mV s⁻¹ are needed to maintain the discharge times on the order of a minutes and adequately reflect a material's performance as recommended by Meryl D. Stoller and Rodney S. Ruoff [45]. It can be seen that the CV curves of electrode in both electrolytes exhibit rectangular shape which indicate ideal supercapacitive behaviour of the electrode. The rectangular shape is retained for Na₂SO₄ electrolyte up to 1.8 V and for KOH up to 1.0 V, which clearly indicate the potential stability window of the both electrolytes without any electrolyte decomposition. However, the CV curves of the electrode in Na₂SO₄ electrolyte showed distortion behaviour at higher voltage in between 1.6 V and 1.8 V. The CV curves of the electrode in different scan rates from 5 mV s⁻¹ to 100 mV s⁻¹ are appeared in Fig. 4. It is interesting to see that even at the high scan rate of 100 mV s⁻¹, the CV curves of electrode still maintains a quasi-rectangular shape, which indicates its excellent rate capability. The electrode in KOH electrolyte at high scan rate showed better rectangular shape as compared in Na₂SO₄ electrolyte which demonstrates the fast ion transports efficiently inside the electrode due to the small ionic size of the K⁺/OH⁻. The rate performance of supercapacitor can be

benefited by enabling the electrolyte ions effectively enter into the pores. At the point when the scan rate increases, the specific capacitance of the carbon fibres electrode decreases.

The CV curve for the electrode with organic electrolyte 1 M TEABF₄ displays a broader rectangular shape without significant distortion which corresponding to an ideal electrochemical double layer capacitive behaviour. In addition, the rectangular shapes are also well-retained even at 100 mV s⁻¹, which indicate a rapid I–V response and fast charge-discharge characteristic of the supercapacitor at higher scan rate. This result clearly indicated that activated carbon fibres electrode showed a higher capacitance and a better reversibility even at higher scan rate. The galvanostatic charge-discharge (GCD) study was carried out at various current densities as illustrated in Fig. 5. The straight lines with clear symmetric triangular shapes with small IR drops are appeared in all the electrolytes which suggesting the electrode in all the electrolytes have excellent reversibility and good Coulombic efficiency. The specific capacitance of carbon fibres electrode was calculated from GCD curve by using equation (1) and the maximum specific capacitance of the electrode is around 161 F g⁻¹, 116 F g⁻¹ and 112 F g⁻¹ in 6 M KOH, 0.5 M Na₂SO₄ and 1 M TEABF₄/AN organic electrolyte, respectively at a current density of 1 A g⁻¹. It is well known that the specific capacitance of the electrode in 6 M KOH showed higher value than electrode in 0.5 M Na₂SO₄ because the ionic size of SO₄²⁻ is around 0.533 nm, it is much higher than OH⁻ ion (0.36–0.42 nm). Although the specific capacitance of electrode in 0.5 M Na₂SO₄ electrolyte showed lower value than that of KOH, the energy delivers from supercapacitor using 0.5 M Na₂SO₄ as electrolyte showed much higher than 6 M KOH due to the higher potential window of the Na₂SO₄ electrolyte (0–1.8 V), the energy density can be calculated as per equation (3).

The narrow potential window of aqueous electrolytes is critical limiting factors for high energy density supercapacitor. In order to increase the energy density of the supercapacitor, organic electrolyte was used due to its higher potential stability window. In this concern, 1 M TEABF₄/AN organic electrolyte have been widely used in the commercial supercapacitor cells. Herein, the electrochemical performance of the activated carbon fibres was also examined by using 1 M TEABF₄/AN organic electrolyte with the potential windows of 0–2.7 V. As can be seen in Fig. 5(c), the charge-discharge curves of the activated carbon fibres electrode in 1 M TEABF₄/AN organic electrolyte exhibited nearly triangular shapes over a wide range of current densities between 0.5 A g⁻¹ and 10 A g⁻¹. The obtained result is clearly demonstrating an ideal supercapacitive behaviour of the electrodes. Besides, very low IR drop was observed which suggesting a very low equivalent series resistance (ESR) of the activated carbon porous fibres in organic electrolyte. It demonstrates the high electrical conductivity with well interconnected macroporous network of carbon fibres with narrow pore size distribution that allows the free transport of the electrolyte ions with minimum internal residence. The activated carbon fibres electrode with high active mass leading (around 10 mg cm⁻²) showed an excellent gravimetric and volumetric capacitances of 112 F g⁻¹ and 74 F cm⁻³ at 1 A g⁻¹ current density, respectively with low ESR of 0.05 V. Furthermore, the gravimetric and volumetric capacitances of 73 F g⁻¹ and 48 F cm⁻³, respectively at high current density of 10 A g⁻¹ demonstrate the high rate capability of the supercapacitor electrodes.

In order to compare as well as justify the electrochemical performance of the indigenous activated carbon fibres in organic electrolyte, the similar electrochemical performance was conducted by using commercial Kuraray YP-50F supercapacitor grade carbon as electrode by adopting the same experimental conditions. The electrochemical performances of ACF and YP-50F supercapacitor electrodes are compared and the results are depicted in

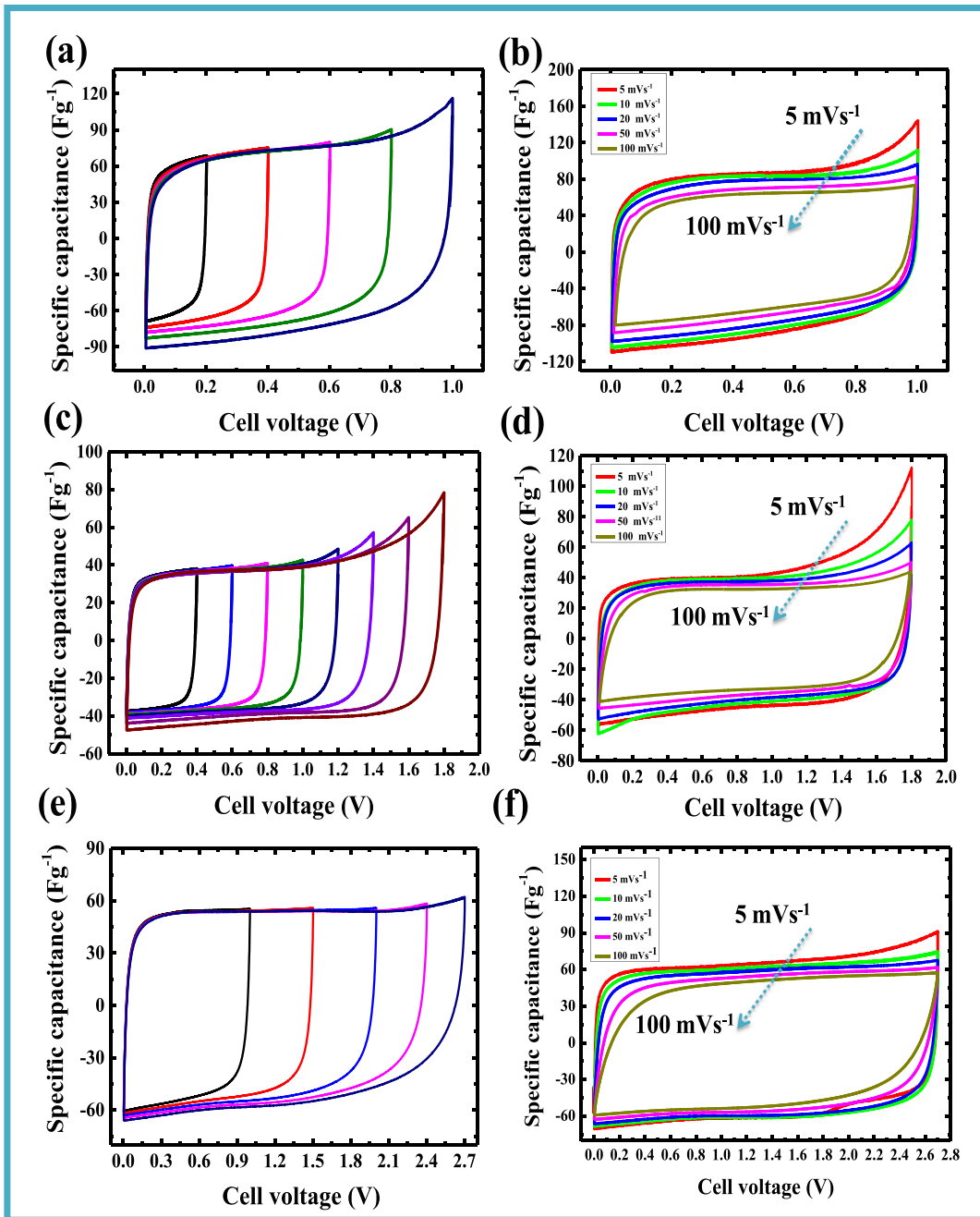


Fig. 4. Electrochemical performances of activated carbon fibres as supercapacitor electrodes by using different electrolytes. (a) CV curves of ACF in 6 M KOH electrolyte at a scan rate of 20 mVs⁻¹, (b) different scan rates in 6 M KOH; (c) CV curves of ACF in 0.5 M Na₂SO₄ at a scan rate of 20 mVs⁻¹, (d) different scan rates in 0.5 M Na₂SO₄; (e) CV curves of ACF in 1 M TEABF₄ at a scan rate of 20 mVs⁻¹, (f) different scan rates in 1 M TEABF₄. (A colour version of this figure can be viewed online.)

Fig. 6. It was observed that activated carbon fibres (ACF) electrodes showed higher gravimetric and volumetric capacitances of 112 Fg⁻¹ and 74 Fcm⁻³ at 1 Ag⁻¹ current density in 2.7 V, respectively as compared with that of commercial YP-50F carbon electrodes (91 Fg⁻¹ & 65 Fcm⁻³ at 1 Ag⁻¹ current density in 2.7 V). Patrice Simon and Yury Gogotsi et al. [46] reported that commercial Kuraray YP-50F using ethyl-methylimidazolium-bis(trifluoromethane-sulfonyl)imide ionic liquid (EMI-TFSI) as electrolyte operated at 3.0 V has received the maximum gravimetric and volumetric specific capacitances of 91 Fg⁻¹ and 45 Fcm⁻³, respectively. This result is well supported to our claim of YP-50F electrodes. As the current density increases, the

capacitances of the both electrodes are decreased due to the internal resistance arising during the fast diffusion of ions into the electrodes. It is very interesting to see that very good rate capability of ACF electrodes with higher capacity retention was observed. This results clearly demonstrated that ACF may provide a very shorten ion diffusion pathway which facilities the rapid ion transfers of TEA⁺/BF₄⁻.

It is worthy to mention here that when the active mass loading of the electrode is increased, the specific capacitance of the electrode is decreased due to the mass transport limitations in high active mass electrodes. In addition, the mechanical strength of the electrodes is also affected. Hence, it is very challenging to fabricate

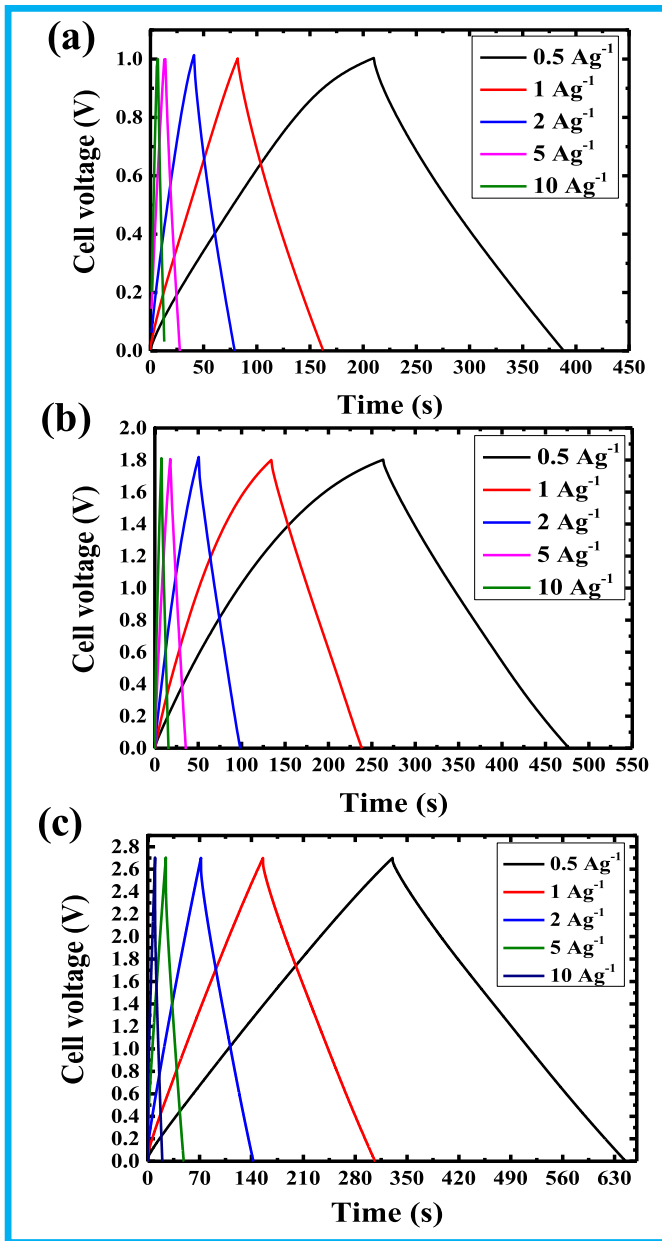


Fig. 5. Galvanostatic charge-discharge curves of ACF at different current densities by using different electrolytes: (a) 6 M KOH, (b) 0.5 M Na₂SO₄, (c) 1 M TEABF₄. (A colour version of this figure can be viewed online.)

the electrode with high active mass loading per cm² with desirable mechanical strength in order to obtain a high energy density supercapacitor electrode without sacrificing power density. For example, the electrode with mass loading of 10 mgcm⁻² is required 10 mA current in order to achieve 1 Ag⁻¹ of current density. In this case, the electrode with high amount of active mass can create a large IR drop due to the ESR. But, the electrode with low active mass loading i.e. 1 mgcm⁻² has obviously low ESR due to the low current 1 mA which corresponding to 1 Ag⁻¹ of current density. These results clearly indicate that the different ESR was observed for the same electrode material with different mass loading. Hence, the mass loading should be taken into account when comparing the data for different electrodes. The above example demonstrate the problems associated with active mass loading of the electrode that corresponding to its gravimetric current densities when compare

the performance of device for the carbon electrode with very different mass loadings. Therefore, it is strongly recommended that when comparing the energy storage devices, a number of parameters such the electrodes areas, electrodes volumes, and active mass loadings of the electrodes should be carefully considered for real applications.

In order to test the series resistance and charge transfer resistance of the supercapacitor electrodes, electrochemical impedance spectroscopy (EIS) was used. The supercapacitor electrodes with low resistance are electrochemically preferred for better commercial device applications. In this concern, all the supercapacitor cells were investigated by EIS. Generally, a supercapacitor behaves like a pure resistor at high frequencies, beside at relatively low frequencies, it behaves like a capacitor. It is well accepted that the diameter of the semicircle at high frequency region reflects the polarization resistance or charge transfer resistance (R_{ct}), and the vertical line at low frequency indicates ideal capacitor behaviour and low diffusion resistance of electrolyte ions. The Nyquist plots of the carbon fibres electrode with different electrolytes such as 6 M KOH, 0.5 M Na₂SO₄ and 1 M TEABF₄/AN are illustrated in Fig. 7(a–c), indicates the impedances in the frequency range between 0.01 Hz and 100 KHz. Nyquist plot shows a vertical straight line perpendicular to the horizontal coordinate for an ideal porous electrode. The Nyquist plot showed straight line for an EDLC at low frequency region. Generally, the more ideal capacitor shows more vertical line. The obtained results showed that all the supercapacitor electrodes have an almost vertical line which indicates ideal supercapacitor behaviour.

However, Nyquist plot can be divided into three parts for real porous electrodes i.e. high, medium and low frequency regions. Nyquist plot shows semicircle and the real axis intercept is the equivalent series resistance (ESR) at high-frequency region [47]. The charge transfer resistance of the electrode materials can be represented via width of the semicircle impedance loop. In addition, same fabrication assembly was used for all the electrodes and hence the contact resistance of the electrodes seems to be identical. However, it shows the different value for the electrodes with respect of the electrolyte used in the supercapacitor cells. The resistance estimation of the carbon electrodes was 0.56 Ω for 6 M KOH, 1.65 Ω for 0.5 M Na₂SO₄ and 1.803 Ω for 1 M TEABF₄/AN, respectively, indicating a good charge-transfer rate. It is observed that the resistance of the carbon electrode in 6 M KOH showed very low as compared to that of Na₂SO₄ as well as 1 M TEABF₄/AN electrolytes because KOH has a very high ionic conductivity as well as high ionic diffusion co-efficient due to smaller ionic size than other two electrolytes. It is well consistent with ion diffusion coefficient of the ions and it is decreasing in the order of KOH ($5.39 \times 10^{-7} \text{ cm}^2 \text{ s}^{-1}$) > Na₂SO₄ ($5.81 \times 10^{-8} \text{ cm}^2 \text{ s}^{-1}$) > TEABF₄ ($3.02 \times 10^{-8} \text{ cm}^2 \text{ s}^{-1}$).

Furthermore, the rate capability of the supercapacitor electrode and the electrochemical long term stability of the electrode in different electrolytes were further investigated as shown in Fig. 8(a–c). The high rate capability of the electrodes in different electrolytes with potential windows between 0 and 2.7 V was investigated and the gravimetric and volumetric capacitance of the supercapacitor electrode are depicted in Fig. 8(a and b). As the current density increases, the capacitance of the electrode in all the electrolytes is decreased due to the internal resistance arising during the fast diffusion of ions into the electrode. Among the electrolytes investigated, very good rate capability of ACF electrode with higher capacity retention was observed in the 0.5 M Na₂SO₄ electrolyte as depicted in Fig. 8(a and b) because the pore structure of the ACF may provide a very shorten ion diffusion pathway which facilitates the rapid ion transfer of Na⁺/SO₄²⁻. From practical point of view, the stability of supercapacitors device upon charge-discharge

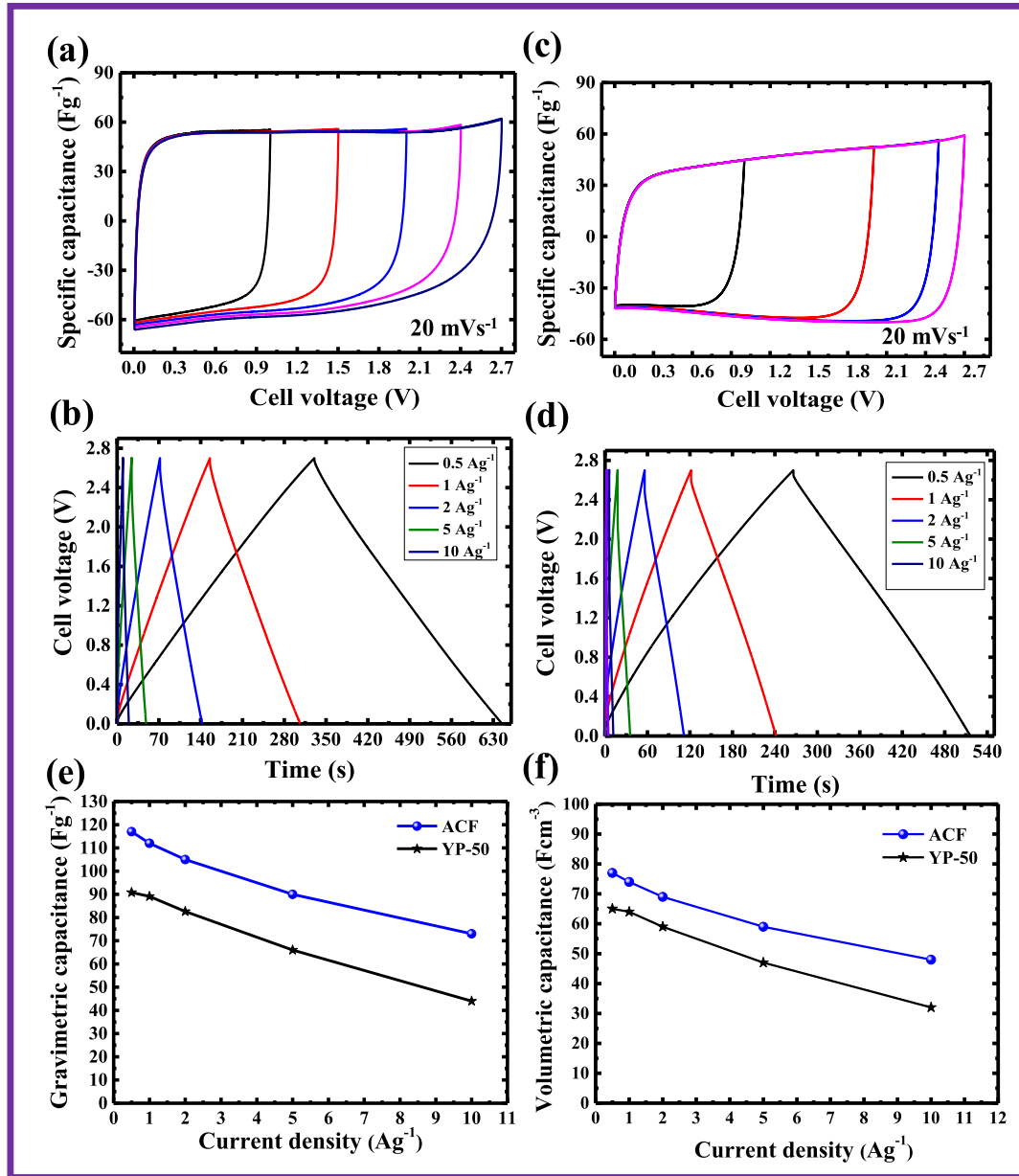


Fig. 6. Comparison of electrochemical performances of activated carbon fibres with commercial Kuraray YP-50F carbon. (a,b) Activated carbon fibres (ACF), (c,d) YP-50F carbon, (e,f) Gravimetric and volumetric capacitance with respect of current density. (A colour version of this figure can be viewed online.)

cycling is another important aspect. The electrode stability was investigated by long-term charge-discharge cycle at current density of 1 Ag^{-1} with a potential window of $0\text{--}2.7 \text{ V}$ by using different electrolytes as shown in Fig. 8(c). It was observed that after 10,000 cycles in different electrolytes system still retains above ~87% of its initial capacitance with less equivalent series resistance (ESR), evidencing the superb robustness of the carbon fibre electrode, at discharge rate of 1 Ag^{-1} . Furthermore, it can be seen from Fig. 8c that the gradual decrease in the capacitance was observed until 2000 cycles and then it is constantly maintained. The initial loss of capacitance may be attributed to the internal resistance (equivalent series resistance (ESR) and/or equivalent distributed resistance (EDR)) of the electrodes due to the thick electrode as observed from the IR drop in the charge-discharge profile in the initial cycles at high current density of 1 Ag^{-1} . After the stabilisation the electrodes up to 2000 cycles, the capacitance is constantly maintained and

consequently the IR drop is also stabilized upon cycling. In addition, it is anticipated that the electrolyte needs a certain number of cycles before it can diffuse into all the available porosity, and because of that, the electric double-layer formation is somewhat hindered at the beginning of the durability test. However, the loss of capacitance in the 1000 and 2000 cycles is around 5% and 10% of the initial capacitance, respectively and then it is reached around maximum of 13% loss of initial capacitance at end of the 10,000 cycles. This similar observation was reported by V. Khomenko et al. [48] and they found that small decrease (15%) of the capacitance observed in the first 2000 cycles is interpreted by a small expand of the electrodes and after this period, the specific capacitance almost remains constant up to 10,000 cycles.

For practical applications, the energy density and power density of the supercapacitor device are the major parameters and it is represented via Ragone plot. Hence, Ragone plot of the symmetric

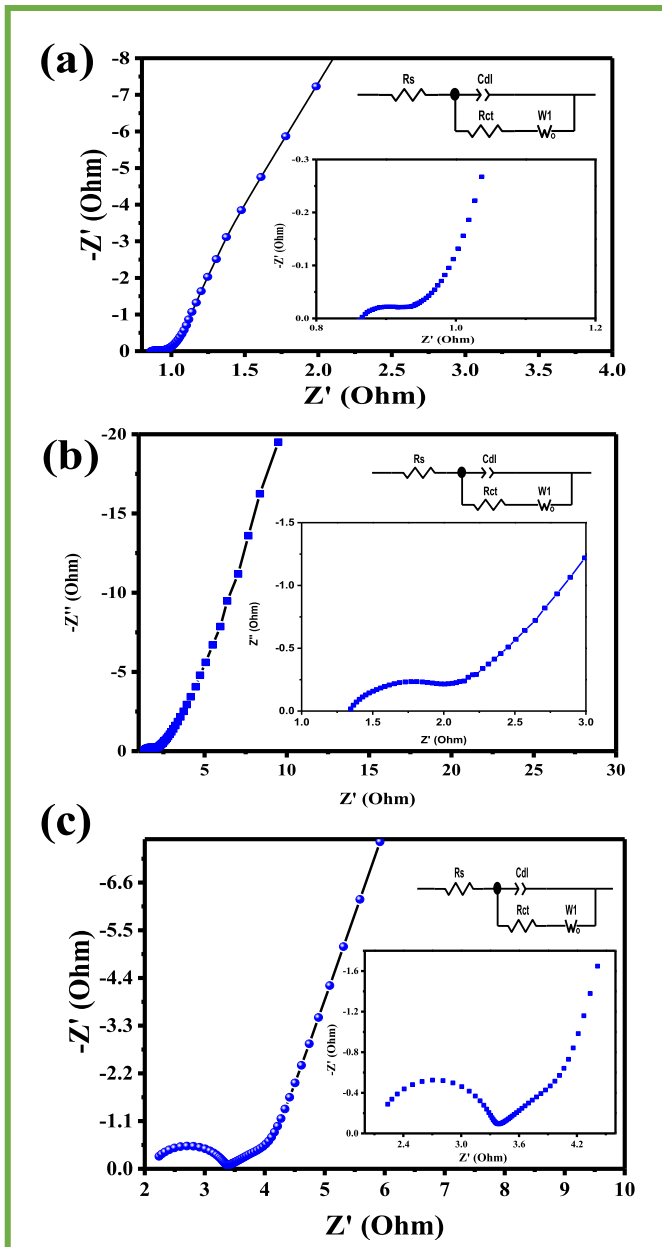


Fig. 7. Comparison of Nyquist plots for symmetric supercapacitor cells in different electrolytes: (a) 6 M KOH, (b) 0.5 M Na_2SO_4 , (c) 1 M TEABF_4 . (A colour version of this figure can be viewed online.)

supercapacitor cell is shown in Fig. 9, which indicates the supercapacitor cell has promising power-energy characteristics. In this study, the high energy density and power density was achieved in the supercapacitor electrodes with mass loading of 10 mg cm^{-2} , which is prerequisite of high mass loading for commercial supercapacitor applications. Of course, the energy and power densities of supercapacitor cells were calculated based only on the total mass of the electrodes.

The gravimetric energy density of ACF increases in the order of $6.2 \text{ Wh kg}^{-1} > 13.4 \text{ Wh kg}^{-1} > 29.5 \text{ Wh kg}^{-1}$, which corresponding to 6 M KOH, 0.5 M Na_2SO_4 and 1 M TEABF_4/AN as electrolyte, respectively as shown in Fig. 9(a). The supercapacitor cell with 1 M TEABF_4/AN organic electrolyte exhibits the highest energy density of around 29.5 Wh kg^{-1} with the corresponding power density of around 10 kW kg^{-1} which showed higher value as compared to

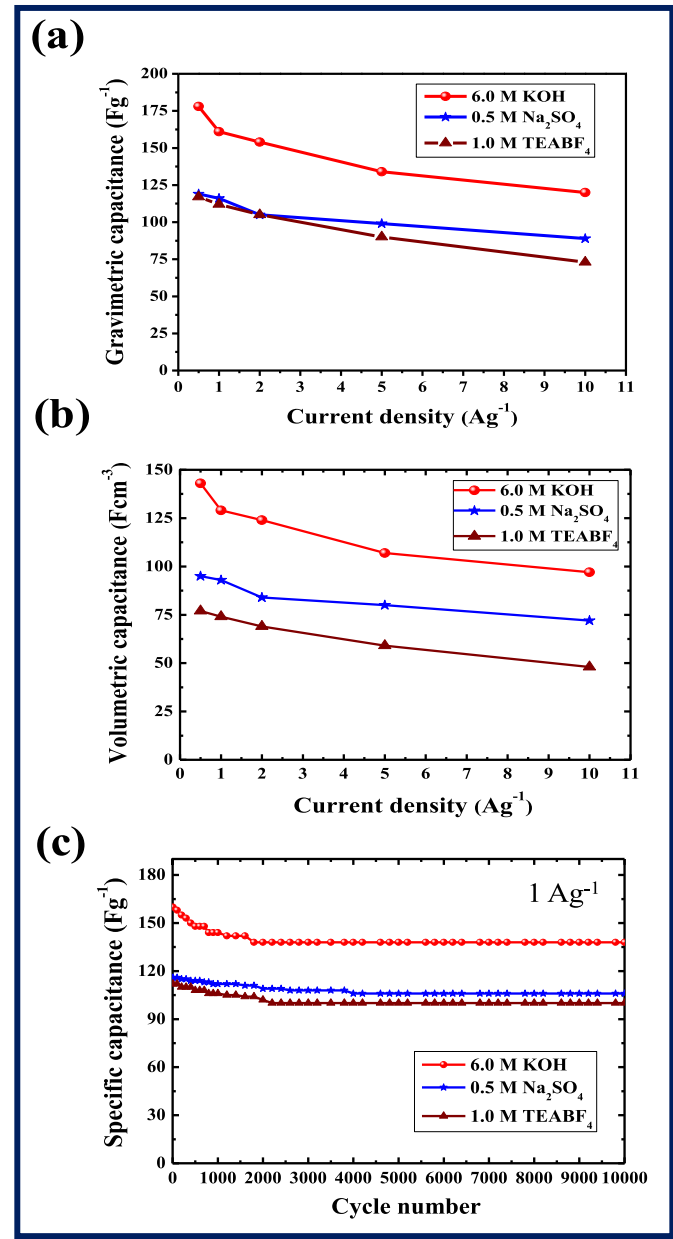


Fig. 8. The rate capability and cycling stability of ACF electrodes in different electrolytes. (a) Gravimetric capacitance at different current densities, (b) Volumetric capacitance at different current densities, (c) Long term cycle stability of ACF electrodes at current density of 1 Ag^{-1} . (A colour version of this figure can be viewed online.)

other carbon based supercapacitor electrodes reported in the literature. For e.g. the obtained energy density value in this study is comparable to those previously reported for other carbon based electrodes, such as graphene material ($\sim 7 \text{ Wh kg}^{-1}$) [49], activated porous carbons ($\sim 6\text{--}10 \text{ Wh kg}^{-1}$) [50], porous carbon shell ($\sim 10 \text{ Wh kg}^{-1}$) [51], Rod-shaped porous carbon ($\sim 17\text{--}20 \text{ Wh kg}^{-1}$) [52], nitrogen-doped porous carbon ($\sim 12\text{--}20 \text{ Wh kg}^{-1}$) [53]. Accordingly, the volumetric energy density Vs power density of the supercapacitor electrodes with different electrolytes is represented in Fig. 9(b). As expected, the organic electrolyte showed a highest volumetric energy density of 19.42 Wh l^{-1} as compared with other electrolytes. The activated carbon fibres electrode exhibited higher volumetric energy density as compared with the carbon-based electrodes reported in the literature as mentioned in Table 1.

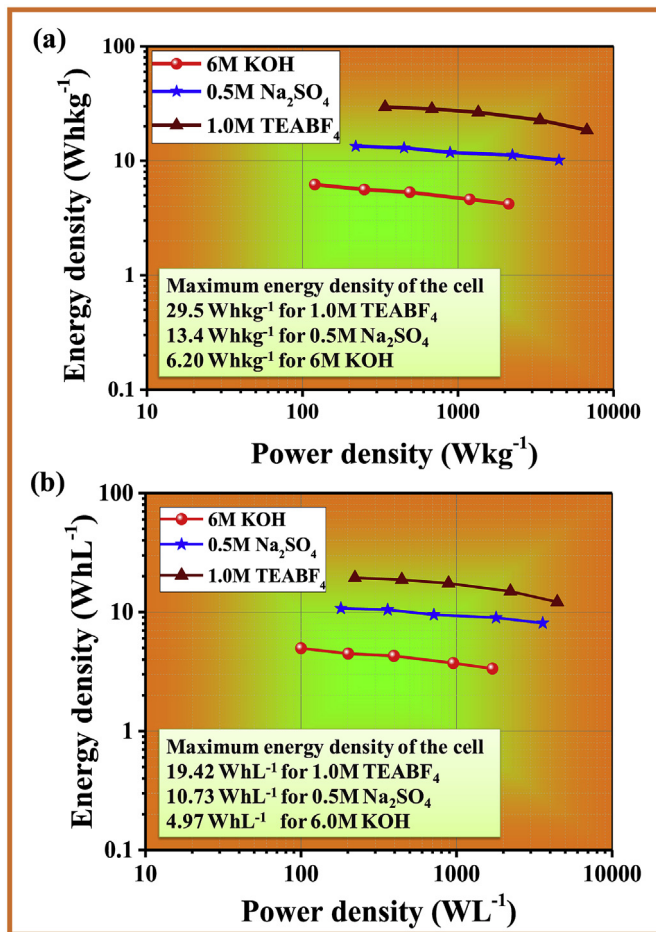


Fig. 9. Ragone plot of the supercapacitor cell in different electrolytes. (a) Gravimetric energy density Vs Power density, (b) Volumetric energy density Vs Power density. (A colour version of this figure can be viewed online.)

3.3. Demonstration of mini-proto-type supercapacitor device

In the practical application, the fabricated activated carbon

fibres based supercapacitor cells were further tested by using mini-proto-type devices as depicted in Fig. 10. The coin cells and Swagelok cells are fabricated and demonstrated by using various devices. In order to increase the capacitance and voltage, a set of the supercapacitor cells were connected in the series and parallel and they were tested. If the supercapacitor coin cells are connected in series, the total voltage is increased as demonstrated by illuminating 40 LED lights in the lantern. When the supercapacitor cells are connected in parallel, the total capacitance is increased as demonstrated by illuminating a high power LED light. A practical approach to combine the supercapacitor (4 coin cells in series, 2.7 V x 4) with a commercial solar cells used in the lantern was developed to integrate self-sustaining power pack as shown in Fig. 10. Importantly, the solar charged supercapacitor can power a commercial solar lantern with 40 light-emitting-diode (LED) lights in the absence of sunlight which demonstrates its potential for efficient conversion of solar energy into electrical energy storage. The efficient capture and convert the sun energy into electrical energy and then stored in the device has showed the utilisation of renewable energy and to produce the economic electricity. These results clearly demonstrate that the solar cells integrated with supercapacitor can consider as an ultrafast next generation energy storage device which can mitigate the energy demand and reduce the cost of the electricity in the near future.

4. Conclusions

A large scale preparation of high surface area activated carbon fibres (ACs, 1550 m² g⁻¹) derived from waste cotton as an economic and abundant renewable natural resource and the fabrication of high-performance supercapacitor electrode was demonstrated. The electrochemical performance and supercapacitive behaviours of carbon fibres electrodes with commercial level mass loading was investigated and the small proto-type supercapacitor devices were demonstrated for practical validity. The supercapacitor performance of the obtained carbon electrode was examined and the carbon material has excellent electrochemical performance, including the larger specific capacitance, good rate capability, higher frequency response, and superb cycling stability in aqueous and non-aqueous electrolytes. The fabricated supercapacitor cells exhibited the maximum gravimetric capacitance of 161 F g⁻¹, 116 F g⁻¹ and 112 F g⁻¹ in 6 M KOH, 0.5 M Na₂SO₄ and 1 M TEABF₄/AN

Table 1

Comparison of the volumetric capacitance and volumetric energy density of ACF with other carbon based electrodes reported in the literature.

S. No.	Supercapacitor Cell	Potential window of electrolyte (V)	Volumetric Capacitance (F/cm ³)	Volumetric Energy Density (Wh/L)	Ref.
1	Bamboo-like Carbon//Bamboo-Like carbon	0.9	2.1	0.24	[54]
2	Boron and Nitrogen-Porous carbon tube bundles//Boron and Nitrogen-Porous carbon tube bundles	1.8	27	12.15	[55]
3	Activated carbon Fibres//Activated carbon Fibres	0.8	27.60	2.50	[56]
4	Activated wood carbon//MnO ₂ @Wood carbon	1.8	14.40	6.40	[57]
5	CNT Fibres//CNT Fibres	0.8	13.50	0.60	[58]
6	Mesoporous carbon sheet-like framework//Mesoporous carbon sheet-like framework	1.6	17.40	6.20	[59]
7	Mesoporous Vanadium Nitride/CNT//Mesoporous Vanadium Nitride/CNT	0.7	7.90	0.54	[60]
8	Ordered Microporous carbon/CNT//Ternary Hybrid Fiber	1.6	23.40	11.30	[61]
9	Hydrogen treated-TiO ₂ @MnO ₂ //Hydrogen treated -TiO ₂ @C	1.8	0.70	0.30	[62]
10	laser-scribed graphene//laser-scribed graphene	3.0	13.2	1.36	[63]
11	Hydrogen annealed graphene//Hydrogen annealed graphene	3.0	23.33	6.59	[64]
12	Commercial Kuraray YP-50F	2.7	65	16.47	Present work
13	Activated Carbon Fibres	1.0 1.8 2.7	129 93 74	4.97 10.73 19.42	Present work Present work



Fig. 10. Demonstration of supercapacitor devices by using activated carbon fibres as economic and scalable supercapacitor electrodes. (A colour version of this figure can be viewed online.)

organic electrolyte, respectively at a current density of 1 A/g. The gravimetric energy density of ACF increases in the order of $6.2 \text{ Whkg}^{-1} > 13.4 \text{ Whkg}^{-1} > 29.5 \text{ Whkg}^{-1}$, which corresponding to 6 M KOH, 0.5 M Na₂SO₄ and 1 M TEABF₄/AN as electrolytes, respectively. The supercapacitor cell with 1 M TEABF₄/AN organic electrolyte exhibits the highest gravimetric energy density of around 29.5 Whkg^{-1} with the corresponding volumetric energy density of around 19.42 Whl^{-1} which showed higher value as compared to other carbon based supercapacitor electrodes reported in the literature. This study highlighted that the mass loading should be taken into account when comparing the data for different electrodes. It also demonstrates the problems associated with active mass loading of the electrode that corresponding to its gravimetric current densities when compare the performance of device for the carbon electrode with very different mass loadings. Therefore, it is strongly recommended that when comparing the energy storage devices, a number of parameters such the electrodes areas, electrodes volumes, and active mass loadings of the electrodes should be carefully considered for real applications. In combination with the low cost and easy fabrication process, the activated porous carbon fibres can be considered as a promising electrode material for supercapacitor practical applications. These results demonstrate the possibility of the integration and hybridizing energy conversion and energy storage and the solar cells integrated with supercapacitor as a next generation clean energy storage device can mitigate the energy demand and reduce the cost of the electricity in the near future.

Acknowledgements

This research work was supported by technical research centre (TRC) project (Ref. No. AI/1/65/ARCI/2014 (c)) sponsored by

Department of Science and Technology (DST), Govt. Of India, New Delhi, India.

Appendix A. Supplementary data

Supplementary data related to this article can be found at <https://doi.org/10.1016/j.carbon.2018.08.052>.

References

- [1] F. Barzegar, A. Bello, J.K. Dangbegnon, N. Manyala, X. Xia, Asymmetric supercapacitor based on activated expanded graphite and pinecone tree activated carbon with excellent stability, *Appl. Energy* 207 (2017) 417–426.
- [2] M. Sevilla, R. Mokaya, Energy storage applications of activated carbons: supercapacitors and hydrogen storage, *Energy Environ. Sci.* 7 (2014) 1250–1280.
- [3] T. Chen, L. Dai, Carbon nanomaterials for high-performance supercapacitors, *Mater. Today* 16 (2013) 272–280.
- [4] Z. Wu, L. Li, J.m. Yan, X.b. Zhang, Materials design and system construction for conventional and new-concept supercapacitors, *Advanced Science* 4 (2017) 1600382.
- [5] M. Canal-Rodríguez, J.A. Menéndez, A. Arenillas, Performance of carbon xerogel-graphene hybrids as electrodes in aqueous supercapacitors, *Electrochim. Acta* 276 (2018) 28–36.
- [6] Z. Chen, K. Liu, S. Liu, L. Xia, J. Fu, X. Zhang, C. Zhang, B. Gao, Porous active carbon layer modified graphene for high-performance supercapacitor, *Electrochim. Acta* 237 (2017) 102–108.
- [7] J.-H. Choi, C. Lee, S. Cho, G.D. Moon, B.-s. kim, H. Chang, H.D. Jang, High capacitance and energy density supercapacitor based on biomass-derived activated carbons with reduced graphene oxide binder, *Carbon* 132 (2018) 16–24.
- [8] J.B. Goodenough, Evolution of strategies for modern rechargeable batteries, *Acc. Chem. Res.* 46 (2013) 1053–1061.
- [9] M. Genovese, H. Wu, A. Virya, J. Li, P. Shen, K. Lian, Ultrathin all-solid-state supercapacitor devices based on chitosan activated carbon electrodes and polymer electrolytes, *Electrochim. Acta* 273 (2018) 392–401.
- [10] K. Naoi, W. Naoi, S. Aoyagi, J.-i. Miyamoto, T. Kamino, New generation - nanohybrid supercapacitor, *Acc. Chem. Res.* 46 (2013) 1075–1083.
- [11] S. Herou, P. Schlee, A.B. Jorge, M. Titirici, Biomass-derived electrodes for

- flexible supercapacitors, *Current Opinion in Green and Sustainable Chemistry* 9 (2018) 18–24.
- [12] X. Kang, H. Zhu, C. Wang, K. Sun, J. Yin, Biomass derived hierarchically porous and heteroatom-doped carbons for supercapacitors, *J. Colloid Interface Sci.* 509 (2018) 369–383.
- [13] Y. Zhao, L.P. Wang, M.T. Sougrati, Z. Feng, Y. Leconte, A. Fisher, M. Srinivasan, Z. Xu, A review on design strategies for carbon based metal oxides and sulfides nanocomposites for high performance Li and Na ion battery anodes, *Advanced Energy Materials* 7 (2017) 1601424.
- [14] Y. Shao, M.F. El-Kady, L.J. Wang, Q. Zhang, Y. Li, H. Wang, M.F. Mousavi, R.B. Kaner, Graphene-based materials for flexible supercapacitors, *Chem. Soc. Rev.* 44 (2015) 3639–3665.
- [15] T. Li, Y. Zuo, X. Lei, N. Li, J. Liu, H. Han, Regulating the oxidation degree of nickel foam: a smart strategy to controllably synthesize active Ni₃S₂ nanorod/nanowire arrays for high-performance supercapacitors, *J. Mater. Chem.* 4 (2016) 8029–8040.
- [16] J. Martínez-Lao, F.G. Montoya, M.G. Montoya, F. Manzano-Agugliaro, Electric vehicles in Spain: an overview of charging systems, *Renew. Sustain. Energy Rev.* 77 (2017) 970–983.
- [17] D. Maamria, K. Gillet, G. Colin, Y. Chamaillard, C. Nouillant, Computation of eco-driving cycles for hybrid electric vehicles: comparative analysis, *Contr. Eng. Pract.* 71 (2018) 44–52.
- [18] M. Safari, Battery electric vehicles: looking behind to move forward, *Energy Pol.* 115 (2018) 54–65.
- [19] Z. Song, X. Zhang, J. Li, H. Hofmann, M. Ouyang, J. Du, Component sizing optimization of plug-in hybrid electric vehicles with the hybrid energy storage system, *Energy* 144 (2018) 393–403.
- [20] X.-L. Su, J.-R. Chen, G.-P. Zheng, J.-H. Yang, X.-X. Guan, P. Liu, X.-C. Zheng, Three-dimensional porous activated carbon derived from loofah sponge biomass for supercapacitor applications, *Appl. Surf. Sci.* 436 (2018) 327–336.
- [21] Q. Xue, J. Sun, Y. Huang, M. Zhu, Z. Pei, H. Li, Y. Wang, N. Li, H. Zhang, C. Zhi, Recent progress on flexible and wearable supercapacitors, *Small* 13 (2017) 1701827.
- [22] J. Deng, M. Li, Y. Wang, Biomass-derived carbon: synthesis and applications in energy storage and conversion, *Green Chem.* 18 (2016) 4824–4854.
- [23] L. Eliad, G. Salitra, A. Soffer, D. Aurbach, Ion sieving effects in the electrical double layer of porous carbon Electrodes: estimating effective ion size in electrolytic solutions, *J. Phys. Chem. B* 105 (2001) 6880–6887.
- [24] P. Xiao, S. Quan, C. Xie, A new supercapacitor and Li-ion battery hybrid system for electric vehicle in ADVISOR, *J. Phys. Conf.* 806 (2017), 012015.
- [25] S. Wang, Z. Ren, J. Li, Y. Ren, L. Zhao, J. Yu, Cotton-based hollow carbon fibers with high specific surface area prepared by ammonia etching for supercapacitor application, *RSC Adv.* 4 (2014) 31300–31307.
- [26] K. Thileep Kumar, G. Sivagaami Sundari, E. Senthil Kumar, A. Ashwini, M. Ramya, P. Varsha, R. Kalaivani, M. Shanmugaraj Andikkadu, V. Kumaran, R. Gnanamuthu, S.Z. Karazhanov, S. Raghu, Synthesis of nanoporous carbon with new activating agent for high-performance supercapacitor, *Mater. Lett.* 218 (2018) 181–184.
- [27] B. Wang, J. Qiu, H. Feng, E. Sakai, T. Komiyama, KOH-activated nitrogen doped porous carbon nanowires with superior performance in supercapacitors, *Electrochim. Acta* 190 (2016) 229–239.
- [28] G. Lin, R. Ma, Y. Zhou, Q. Liu, X. Dong, J. Wang, KOH activation of biomass-derived nitrogen-doped carbons for supercapacitor and electrocatalytic oxygen reduction, *Electrochim. Acta* 261 (2018) 49–57.
- [29] W. Zuo, R. Li, C. Zhou, Y. Li, J. Xia, J. Liu, Battery-supercapacitor hybrid devices: recent progress and future prospects, *Advanced Science* 4 (2017) 1600539.
- [30] C. Liu, J. Liu, J. Wang, J. Li, R. Luo, J. Shen, X. Sun, W. Han, L. Wang, Electrospun mulberry-like hierarchical carbon fiber web for high-performance supercapacitors, *J. Colloid Interface Sci.* 512 (2018) 713–721.
- [31] S. Lu, Y. Song, K. Guo, X. Chen, J. Xu, L. Zhao, Effect of aqueous electrolytes on the electrochemical behaviors of ordered mesoporous carbon composites after KOH activation as supercapacitors electrodes, *J. Electroanal. Chem.* 745 (2015) 80–87.
- [32] Y. Xiao, C. Long, M.-T. Zheng, H.-W. Dong, B.-F. Lei, H.-R. Zhang, Y.-L. Liu, High-capacity porous carbons prepared by KOH activation of activated carbon for supercapacitors, *Chin. Chem. Lett.* 25 (2014) 865–868.
- [33] J. Yang, L. Zou, Graphene films of controllable thickness as binder-free electrodes for high performance supercapacitors, *Electrochim. Acta* 130 (2014) 791–799.
- [34] C.H. Ng, H.N. Lim, S. Hayase, I. Harrison, A. Pandikumar, N.M. Huang, Potential active materials for photo-supercapacitor: a review, *J. Power Sources* 296 (2015) 169–185.
- [35] E. Hür, A. Arslan, New electrode active materials for supercapacitors: pencil graphite electrode coated with cobalt ion doped poly(3-methylthiophene) and poly(3,4-ethylenedioxythiophene), *Synth. Met.* 193 (2014) 81–88.
- [36] N. Blomquist, T. Wells, B. Andres, J. Bäckström, S. Forsberg, H. Olin, Metal-free supercapacitor with aqueous electrolyte and low-cost carbon materials, *Sci. Rep.* 7 (2017) 39836.
- [37] M. Vangari, T. Pryor, L. Jiang, Supercapacitors: review of materials and fabrication methods, *J. Energy Eng.* 139 (2013) 72–79.
- [38] M. Karthik, E. Redondo, E. Goikolea, V. Roddatis, R. Mysyk, Large-scale hydrothermal synthesis of hierarchical mesoporous carbon for high-performance supercapacitors, *Energy & Environment Focus* 4 (2015) 201–208.
- [39] M. Karthik, E. Redondo, E. Goikolea, R. Vladimir, S. Doppiu, R. Mysyk, Effect of mesopore ordering in otherwise similar micro/mesoporous carbons on the high-rate performance of electric double-layer capacitors, *J. Phys. Chem. C* 118 (2014) 27715–27720.
- [40] L.B. Hu, J.W. Choi, Y. Yang, S. Jeong, F. La Mantia, L.F. Cui, Y. Cui, Highly conductive paper for energy-storage devices, *Proc. Natl. Acad. Sci. U.S.A.* 106 (2009) 21490.
- [41] Wenhua Zuo, Pan Xu, Yuanyuan Li, Jinping Liu, Direct growth of bismuth film as anode for aqueous rechargeable batteries in LiOH, NaOH and KOH electrolytes, *Nanomaterials* 5 (2015) 1756–1765.
- [42] Dhanya Puthusseri, Vanchiappan Aravindan, Srinivasan Madhavi, Satishchandra Ogale, 3D micro-porous conducting carbon beehive by single step polymer carbonation for high performance supercapacitors: the magic of in situ porogen formation, *Energy Environ. Sci.* 7 (2014) 728–735.
- [43] Y. Gogotsi, P. Simon, True performance metrics in electrochemical energy storage, *Science* 334 (2011) 917–918.
- [44] H. Wang, C.M.B. Holt, Z. Li, X. Tan, B.S. Amirkhiz, Z. Xu, et al., Graphene-nickel cobaltite nanocomposite asymmetrical supercapacitor with commercial level mass loading, *Nano Research* 5 (2012) 605–617.
- [45] Meryl D. Stoller, Rodney S. Ruoff, Best practice methods for determining an electrode material's performance for ultracapacitors, *Energy Environ. Sci.* 3 (2010) 1294–1301.
- [46] Celine Largeot, Cristelle Portet, John Chmiola, Pierre-Louis Taberna, Yury Gogotsi, Patrice Simon, Relation between the ion size and pore size for an electric double layer capacitor, *J. Am. Chem. Soc.* 130 (2008) 2730–2731.
- [47] P.M. Gomadam, J.W. Weidner, Analysis of electrochemical impedance spectroscopy in proton exchange membrane fuel cells, *Int. J. Energy Res.* 29 (2005) 1133–1151.
- [48] V. Khomenko, E. Raymundo-Pinero, F. Béguin, A new type of high energy asymmetric capacitor with nanoporous carbon electrodes in aqueous electrolyte, *J. Power Sources* 195 (2010) 4234–4241.
- [49] Y. Tao, X. Xie, W. Lv, D.-M. Tang, D. Kong, Z. Huang, H. Nishihara, T. Ishii, B. Li, D. Golberg, Towards ultrahigh volumetric capacitance: graphene derived highly dense but porous carbons for supercapacitors, *Sci. Rep.* 3 (2013) 2975–2982.
- [50] D.W. Wang, F. Li, M. Liu, G.Q. Lu, H.M. Cheng, 3D aperiodic hierarchical porous graphitic carbon material for high-rate electrochemical capacitive energy storage, *Angew. Chem. Int. Ed.* 47 (2008) 373–376.
- [51] W. Yang, F. Ding, L. Sang, Z. Ma, G. Shao, Template free synthesis of ultrathin porous carbon shell with excellent conductivity for high rate supercapacitors, *Carbon* 111 (2017) 419–427.
- [52] K. Wang, Y. Cao, X. Wang, M.A. Castro, B. Luo, Z. Gu, J. Liu, J.D. Hoefelmeyer, Q. Fan, Rod-shape porous carbon derived from aniline modified lignin for symmetric supercapacitors, *J. Power Sources* 307 (2016) 462–467.
- [53] C. Long, J. Zhuang, Y. Xiao, M. Zheng, H. Hu, H. Dong, B. Lei, H. Zhang, Y. Liu, Nitrogen-doped porous carbon with an ultrahigh specific surface area for superior performance supercapacitors, *J. Power Sources* 310 (2016) 145–153.
- [54] Y. Sun, R.B. Sills, X. Hu, Z.W. Seh, X. Xiao, H. Xu, W. Luo, H. Jin, Y. Xin, T. Li, Z. Zhang, J. Zhou, W. Cai, Y. Huang, Y. Cui, A bamboo-inspired nanostructure design for flexible, foldable, and twistable energy storage devices, *Nano Lett.* 15 (2015) 3899–3906.
- [55] Jing Zhao, Yiju Li, Guiling Wang, Wei Tong, Liu Zheng, Kui Cheng, Ke Ye, Kai Zhu, Dianxue Cao, Zhuangjun Fan, Enabling high-volumetric-energy-density supercapacitors: designing open, low-tortuosity heteroatom-doped porous carbon-tube bundle electrodes, *J. Mater. Chem. 5* (2017) 23085–23093.
- [56] W. Ma, S. Chen, S. Yang, W. Chen, W. Weng, M. Zhu, Bottom-up fabrication of activated carbon fiber for all-solid-state supercapacitor with excellent electrochemical performance, *Applied Materials Interfaces* 8 (2016) 14622–14627.
- [57] C. Chen, Y. Zhang, Y. Li, J. Dai, J. Song, Y. Yao, Y. Gong, I. Kierzewski, J. Xieand L. Hu, All-wood, low tortuosity, aqueous, biodegradable supercapacitors with ultra-high capacitance, *Energy Environ. Sci.* 10 (2017) 538–545.
- [58] P. Xu, T.L. Gu, Z.Y. Cao, B.Q. Wei, J.Y. Yu, F.X. Li, J.H. Byun, W.B. Lu, Q.W. Li, Carbon nanotube fiber based stretchable wire-shaped supercapacitors, *Advanced Energy Materials* 4 (2014) 13007591.
- [59] Q. Wang, J. Yan, T. Wei, J. Feng, Y. Ren, Z. Fan, M. Zhang, X. Jing, Two-dimensional mesoporous carbon sheet-like framework material for high-rate supercapacitors, *Carbon* 60 (2013) 481–487.
- [60] X. Xiao, X. Peng, H. Jin, T. Li, C. Zhang, B. Gao, B. Hu, K. Huo, J. Zhou, Free-standing mesoporous VN/CNT hybrid electrodes for flexible all-solid-state supercapacitors, *Adv. Mater.* 25 (2013) 5091–5097.
- [61] X. Cheng, J. Zhang, J. Ren, N. Liu, P. Chen, Y. Zhang, J. Deng, Y. Wang, H. Peng, Design of a hierarchical ternary hybrid for a fiber-shaped asymmetric supercapacitor with high volumetric energy density, *J. Phys. Chem. C* 120 (2016) 9685–9691.
- [62] X. Lu, M. Yu, G. Wang, T. Zhai, S. Xie, Y. Ling, Y. Tong, Y. Li, H-TiO₂@MnO₂/H-TiO₂ core–shell nanowires for high performance and flexible asymmetric supercapacitors, *Adv. Mater.* 25 (2013) 267–272.
- [63] M. El-Kady, V. Strong, S. Dubin, B. Kaner, Laser scribing of high-performance and flexible graphene-based electrochemical capacitors, *Science* 335 (2012) 1326–1330.
- [64] H. Yang, S. Kannappan, A.S. Pandian, J.H. Jang, Y. Sung Lee, W. Lu, Graphene supercapacitor with both high power and energy density, *Nanotechnology* 28 (2017) 445401.